



INTERNATIONAL INSTITUTE OF WELDING

A world of joining experience

## Application studies for the fatigue strength improvement of welded structures by high-frequency mechanical impact (HFMI) treatment

Halid Yildirim<sup>a,1</sup>, Martin Leitner<sup>b,2</sup>, Gary Marquis<sup>a,c</sup>

Michael Stoschka<sup>b</sup>, Zuheir Barsoum<sup>c,d</sup>

<sup>a</sup>Aalto University, Department of Applied Mechanics, Finland

<sup>b</sup>Mechanical Engineering, Montanuniversität Leoben, Leoben, Austria

<sup>c</sup>Department of Aeronautical & Vehicle Engineering, KTH-Royal Institute of Technology, Stockholm, Sweden

<sup>d</sup>Department of Aerospace Engineering,

<sup>d</sup> Khalifa University of Science, Technology and Research Abu Dhabi, UAE

<sup>1</sup>halid.yildirim@aalto.fi

<sup>2</sup>martin.leitner@unileoben.ac.at

Delegation of Finland

Delegation of Austria

Delegation of Sweden

Delegation of UAE

IIW Document XIII-WG2-144-15

### Abstract

In 2013, the development of a new guideline for the design of high-frequency mechanical impact (HFMI) treatment was presented. The proposed design guidelines were made based on the fatigue data of axially-loaded welded joints which were manufactured from high-strength steels. All the S-N curves were shown to be conservative with respect to the existing fatigue data for laboratory-scale specimens of longitudinal, transverse, and butt welds.

In reality, structures in civil, offshore, mechanical engineering and ship industries generally include large-scale and more complicated components rather than laboratory-scale specimens. Therefore, this paper firstly presents the validation of design proposals by considering fatigue data sets for large-scale welded structures. In total, 62 fatigue data points for bridge, crane and beam-like components are reported, in which the yield strength varies from 250 to 725 MPa, and stress ratio varies from -1 to 0.56. Validations are then extended also for cover plates by performing fatigue tests of 23 weld details both in as-welded and HFMI-treated cases for the use of crane industry. Both the extracted and obtained fatigue data are found to be in good agreement with the previously-proposed design guidelines.

**Keywords:** high-frequency mechanical impact (HFMI), large-scale structures, fatigue strength improvement, high-strength steels, light-weight design

## Nomenclature

$f_y$	Yield strength
FAT	The IIW fatigue class, i.e. the nominal or effective notch stress range in mega pascals corresponding to 95% survival probability at $2 \times 10^6$ cycles to failure (a discrete variable with 10-15% increase in stress between steps)
HFMI	High-frequency mechanical impact
NS	Nominal stress
SHSS	Structural hot spot stress
ENS	Effective notch stress
$K_t$	Effective notch stress concentration factor
$L$	Length
$m_1$	Slope of the S-N line for stress cycles above the knee point
$m_2$	Slope of the S-N line for stress cycles below the knee point
$R$	Stress ratio ( $\sigma_{min} / \sigma_{max}$ )
$N$	Number of cycles
$t$	Plate thickness
$\rho_f$	Fictitious notch radius

## 1 Introduction

In the literature, several thermal and mechanical post-weld treatment techniques have been recommended to overcome the fatigue failure issues of welded joints [1]. These techniques can be generally divided into two groups: (i) weld geometry improvement methods and (ii) residual stress methods; in which grinding, remelting and special welding techniques can be considered in the former group, whereas peening, overloading and stress relieving methods can be accounted for the latter group.

For the weld geometry improvement methods, the first aim is to remove or reduce the size of the weld toe flaws which may result in an extended crack initiation phase of the fatigue life. The second aim is to reduce the local stress concentration due to the weld profile by achieving a smooth transition between the plate and the weld face. For the residual stress methods, on the other hand, the aim is to eliminate the high tensile residual stress in the weld toe region and/or induce compressive residual stresses at the weld toe. Particularly, peening techniques are relatively known to be beneficial and they have been accessed in the design regulations and guidelines [2] [3] [4]. Amongst others, one such peening technique called high-frequency mechanical impact (HFMI) treatment has developed as a novel, reliable and effective post-weld treatment method for increasing the fatigue strength of welded joints.

In 2013, after a comprehensive literature review of existing fatigue data and an experimental round robin study, Marquis et al. [5] proposed the guidelines for improving the fatigue strength improvement of welded structures by HFMI treatment. In the meantime, a companion document on the procedures and quality assurance was also published by Marquis and Barsoum [6]. The proposal is considered to apply for steel structures of plate thicknesses from 5 to 50 mm and for yield strengths ranging from 235 to 960 MPa.

The guideline basically proposes characteristic fatigue strength values as a function of the



material yield strength. Namely, additional one (1) fatigue class increase in strength (about 12.5%) for every 200 MPa increase in static yield strength is allowed. This so-called stepwise increase is shown in Figure 1 with reference to the same as-welded detail and improved weld detail by the existing International Institute of Welding (IIW) recommendations [7]. With this suggestion, a four (4) fatigue class increase in strength has been defined for joints fabricated from  $235 < f_y \leq 355$  MPa steel with respect to the nominal fatigue class in the as-welded condition. This increase has been extended up to an eight (8) fatigue class improvement for  $f_y > 950$  MPa steel. All the fatigue classes are defined for  $N = 2 \times 10^6$  cycles and assume an S-N slope of  $m_1 = 5$  for HFMI-treated welds. It is clear from the Figure 1 that HFMI allows larger improvement factors in comparison to the IIW recommendations, where only a two (2) and three (3) fatigue class increase for  $355 \text{ MPa} < f_y$  and  $f_y > 355$  MPa with a slope of  $m_1 = 3$  are allowed, respectively. The stepwise approach has been further implemented for the local approaches. These local approaches are the structural hot-spot stress (SHSS) and the effective notch stress (ENS) as defined by the Commission XIII-Fatigue of Welded Components and Structures of the IIW. In terms of the SHSS, two sets of characteristic S-N curves have been suggested according to load carrying properties, namely for non-load carrying and load-carrying welds. Additionally, one set of S-N curves has been proposed for all the three types of geometries in the ENS method. All of the proposals in the guideline have been shown to be conservative with respect to the existing fatigue data points for longitudinal attachments, cruciform welds and butt joints. The included test data are mostly obtained at constant amplitude loading of  $R \leq 0.15$ . Limited data for other R-ratios and variable amplitude testing have also been also studied with respect to the proposed fatigue design recommendations [8].

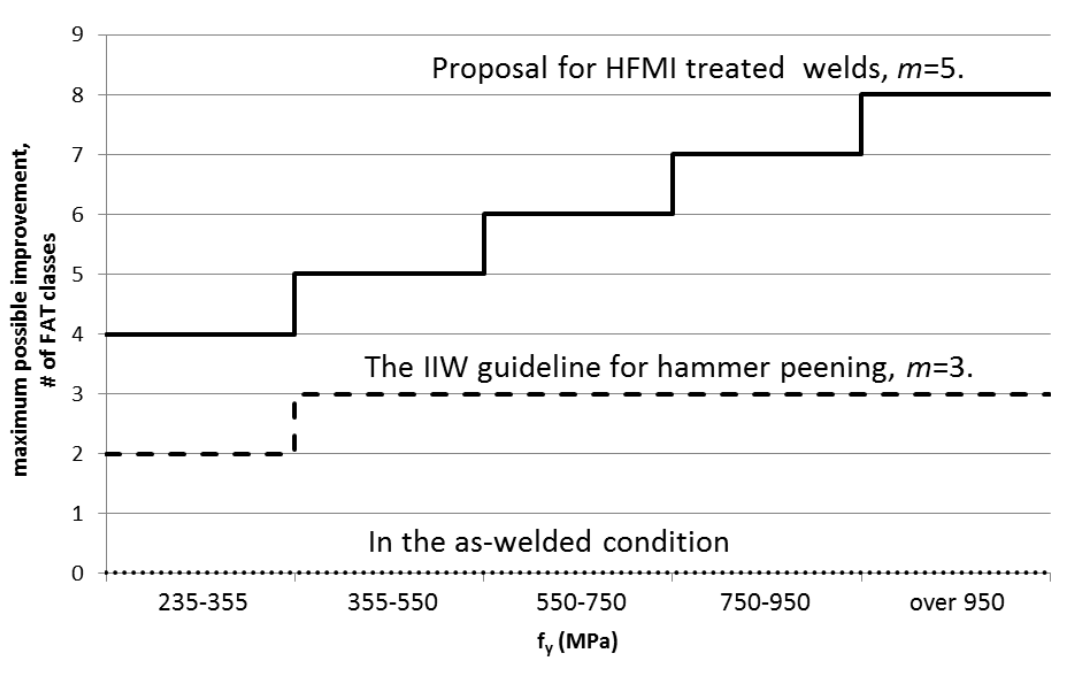


Figure 1: Proposed maximum increases in the number of FAT classes as a function of  $f_y$  from [7].



In practice, on the other hand, structures in civil, offshore, mechanical engineering and ship industries generally composed of large-scale and more complicated components, such as bridges, cranes, platforms, excavators etc. Scale effects are a concern, since welds in large-scale structures tend to have higher tensile residual stresses due to the welding and fabrication process, and higher local notch effects. Therefore, the aim of this paper is to present a validation of the design proposals by considering fatigue data sets for the use of large-scale structures. Validation will be firstly done with the extracted fatigue data obtained for bridge, crane and beam like components, and then it will be demonstrated by fatigue tests performed for a typical cover-plate sample used in crane industry. The extracted fatigue data include various yield strengths ( $250 \leq f_y \leq 725$  MPa) and stress ratios ( $-1 \leq R \leq 0.56$ ). For the experimental fatigue testing part, on the other hand, a yield strength of  $f_y = 900$  MPa high-strength steel has been considered under constant amplitude loading of  $R = 0.1$ .

## 2 Methods

### 2.1 The existing fatigue data for large-scale structures

#### 2.1.1 The extraction method

The authors were able to identify five publications containing fatigue data for welded large-scale structures improved by HFMI treatment [9]. The extracted fatigue data points were re-analysed in this study whereas detailed geometry descriptions can be found in the original studies [2] [10] [11] [12] [13] or in Yıldırım et al. [9]. Table 1 shows the structure and weld detail type, material yield strength, HFMI treatment method, and R-ratio for each data set. In the original works, some of the structures contained multiple weld details. Therefore, total number of the weld detail in series are also reported herein. Many of the studies provided fatigue data explicitly, in which stress ranges and cycles to failure can be found in tables. However, when the references reported fatigue data only as points on a graph, they were extracted from the S-N plots using open source software. This was not considered to introduce significant errors in the results or conclusion. Below, the investigations are mainly separated in two sections based on their component geometries and then briefly explained.

Table 1: Extracted experimental fatigue data for HFMI-treated large structures.

Reference	Steel type	$f_y$ [MPa]	treatment method	structure/weld detail	number of weld detail in series	stress ratio
[10]	S690	$690^b$	UIT	crane/stiffener	9	0.5 and -1
[2]	345W	$407^a$	UIT	beam/cover-plate	15	$0.04 < R \leq 0.53$
[2]	345W	$407^a$	UIT	beam/stiffener	19	$0.04 < R \leq 0.55$
[2]	690W	$725^a$	UIT	beam/stiffener	9	$0.32 < R \leq 0.56$
[11]	KA36	$355^b$	UP	beam/stiffener	2	0
[12]	A36	$250^b$	UIT	cover-plate	6	not reported
[13]	S355	$430^a$	UP	cover-plate	5	0.1

<sup>a</sup> measured  $f_y$

<sup>b</sup> nominal  $f_y$  [14]



### 2.1.2 Beam structures

In a detailed German project called "FOSTA", Khulmann et al. [10] conducted fatigue testing using both small and large-scale components. For the large-scale tests, they considered beam like structures for a bridge structure. A single component included only one HFMI-treated weld detail which was joined in the middle of the span. The yield strength was  $f_y = 690$  MPa and tests were performed at 0.5 and -1 R-ratios. The overall length of the beam-type test component was 4,000 mm.

In another study concerning to the fatigue of bridge details, Roy and Fisher [2] experimentally investigated the fatigue performance of HFMI-treated beam structures subjected to four-point bending. The investigation was valuable since they included data from full-size structures. Large-scale rolled and built-up ferrite-steel beams having  $f_y$  of 366 to 435 MPa and 725 to 760 MPa were fabricated. The welded details included transverse welds at the cover-plate terminus and at the transverse stiffener to tension flange joint. Namely, a single component included two types of weld details with various numbers. HFMI treatment were applied at all the critical weld toe regions. Constant amplitude tests were performed using various stress ratios from  $R = 0$  to  $R = 0.56$  and with stress ranges between 52 and 201 MPa.

Deguchi et al. [11] studied HFMI's benefits to ship structures using one meter beam components subjected to three-point bending. Excessive compressive pre-loading corresponding to the material yield strength was applied after the treatment. Then, fatigue tests were carried out. The material  $f_y$  was 355 MPa and applied stress ratio was  $R = 0$ .

### 2.1.3 Cover-plate specimens

Another interesting study was investigated by Vilhauer et al. [12] on welded cover-plates subjected to three-point bending. Fatigue testing of cover-plates with post-installed tensioned bolts, and a combination of HFMI treatment and bolting were performed. The material was A36 with  $f_y=250$  MPa. Since the applied R-ratio was not reported in the original paper, it can not be shown in Table 1.

Lotsberg et al. [13] have presented the axial fatigue testing of full size fillet welded doubling plates. The region of high nominal stress was 1,800x500 mm. The work showed fatigue test results of as-welded, grinded and HFMI-improved specimens. The paper also presented alternative S-N curves for the improved details.

## 2.2 Application to an industrial crane framework

Lightweight designs of welded high-strength steel frameworks are common in mobile crane industry [15]. One way of achieving this aim is to apply post-weld treatment techniques [16]. Therefore, fatigue testing of samples for a high-performance harvester crane was investigated following the application of HFMI-treatment.

### 2.2.1 Evaluation of the fatigue critical region

Preliminary finite element analyses were performed to evaluate global and local stress conditions of the considered crane structure. For the global model depicted in Figure 2, it has been previously shown that there is no distinctive differences in the resulting stress state



for shell and solid elements [17]. On the other hand, modelling with shell elements offers the possibility to efficiently optimize the plate thickness for lightweight design without huge effort. Nevertheless, in this study, solid elements were used for analysing the highly-stressed structural details since they have been primarily suggested for such complex geometries [18]. The resulting plot for von-Mises stress state of the global solid model showed that one of the stress critical locations was at the end-of-seam detail at the upper shell of the crane, see Figure 2. Further on, red-marked region was also investigated in detail considering the sub-modelling technique [19]. As an outcome for this study, the authors decided to perform experimental investigations on the cover-plate, in which the end-of-seam detail was located. It is worth to mention that the corresponding plot in sub-figure of Figure 2 exhibits a different contour plot limit to highlight the end-of-seam stress concentration. While modelling the weld toe region, the IIW recommendations and best practice rules were followed for performing the notch stress analyses of welded joints [20].

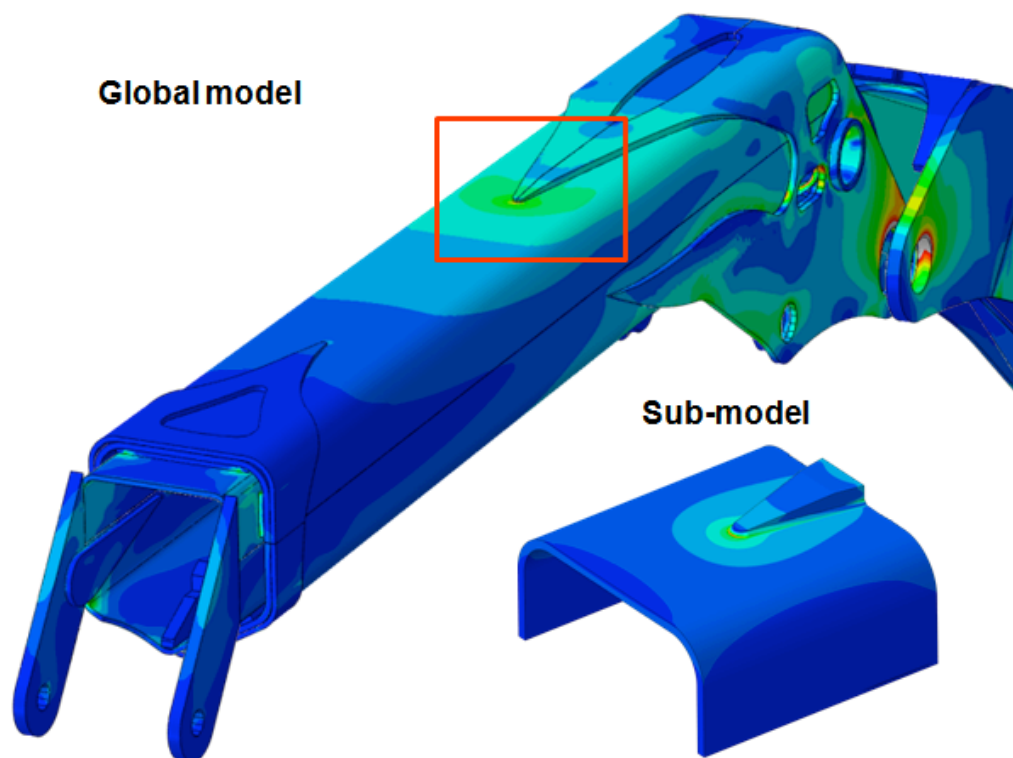


Figure 2: Finite element analyses of the crane by global and sub-model technique from Leitner et al.[17].

### 2.2.2 Manufacturing and fatigue testing of cover-plates

For the experimental analysis of the selected structural detail, a comparable end-of-seam specimen, which exhibits the same local weld seam geometry and plate thickness as in the framework, was designed, see Figure 3. In the current study, twenty-three samples of cover-plates were fabricated from S900 high-strength steel. The chemical composition and conventional material properties are detailed in Table 2. The specimens were manufactured



by an automated welding robot and eight of them were improved by HFMI treatment, see Figure 4. For the treatment parameters, air-pressure was 6 bar, pin frequency was 90 Hz and pin radius was 2 mm. All of the fatigue tests were performed at a constant stress ratio of  $R = 0.1$ .

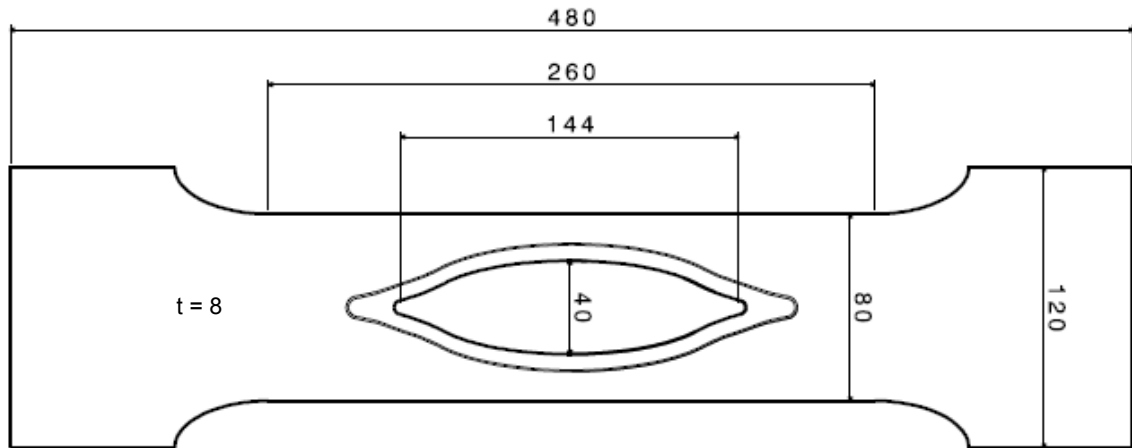


Figure 3: Geometry of the end-of-seam specimen, dimensions in mm.

### 2.2.3 Pseudo-inverse approach to assess operation loads

Due to the highly dynamic working sequences and steady changing environmental conditions, investigation of the operation loads was essential for the fatigue assessment. Evaluation of the service loads at the crane-end was facilitated according to strain gauge measurements at specific positions of the crane and the use of pseudo-inverse approach [21] [22], see Figure 5. In this method, a certain number of numerical calculations to investigate the local stress conditions for every combination of crane position and loading condition are necessary dependent on the degree of freedoms of the crane system. This database acts as principle for the pseudo-inverse matrix by which the re-calculation of the strain gauge to the acting force values in each direction at the crane-end was performed.

### 2.3 HFMI design curves

The comparisons of the fatigue data points obtained from both the literature and tests were performed according to FAT values proposed for the NS and the ENS approaches, as presented by Marquis et al. [5]. In the case of NS based assessment, FAT values have been previously-suggested for each type of weld detail [7] and these values were considered for a particular weld detail in a large-scale component. For the ENS system, however, only one set of FAT values has been proposed.

It is worth to mention that FAT values have been based on the data obtained at a stress ratio of  $R = 0.1$ , and they have been considered to be valid for  $R \leq 0.15$ . In the case of





Figure 4: HFMI-treatment at weld toe of end-of-seam specimens

$$\begin{array}{l}
 F_X = \begin{pmatrix} 1 \\ 0 \\ 0 \end{pmatrix} \longrightarrow \varepsilon_X = \begin{pmatrix} \varepsilon_{1,X} \\ \varepsilon_{2,X} \\ \varepsilon_{3,X} \end{pmatrix} \\
 F_Y = \begin{pmatrix} 0 \\ 1 \\ 0 \end{pmatrix} \longrightarrow \varepsilon_Y = \begin{pmatrix} \varepsilon_{1,Y} \\ \varepsilon_{2,Y} \\ \varepsilon_{3,Y} \end{pmatrix} \\
 F_Z = \begin{pmatrix} 0 \\ 0 \\ 1 \end{pmatrix} \longrightarrow \varepsilon_Z = \begin{pmatrix} \varepsilon_{1,Z} \\ \varepsilon_{2,Z} \\ \varepsilon_{3,Z} \end{pmatrix}
 \end{array}
 \left. \vphantom{\begin{array}{l} F_X \\ F_Y \\ F_Z \end{array}} \right\}
 \begin{pmatrix} F_X(t) \\ F_Y(t) \\ F_Z(t) \end{pmatrix} = \text{Pseudoinv} \begin{bmatrix} \varepsilon_{1,X} & \varepsilon_{1,Y} & \varepsilon_{1,Z} \\ \varepsilon_{2,X} & \varepsilon_{2,Y} & \varepsilon_{2,Z} \\ \varepsilon_{3,X} & \varepsilon_{3,Y} & \varepsilon_{3,Z} \end{bmatrix} \cdot \begin{pmatrix} \varepsilon_{1,\text{measurement}}(t) \\ \varepsilon_{2,\text{measurement}}(t) \\ \varepsilon_{3,\text{measurement}}(t) \end{pmatrix}$$

Figure 5: Pseudo-inverse approach for re-calculation of acting forces at the end of the crane structure

Table 2: Conventional material data

## a. Chemical composition

Steel type	C	Si	Mn	P	S	Al	Nb	V	Ti	Mo	B
S900	0.18	0.50	2.10	0.020	0.008	0.020	0.08	0.15	0.24	0.80	0.005

[%] ladle analysis, maximum values

## b. Mechanical properties (reported minimum values)

Steel type	$R_{p0.2}$ in MPa	$R_m$ in MPa	Elongation in %	Impact strength J at $-20^\circ\text{C}$
S900	900	930	10	27

other types of stress ratios, on the other hand, minimum FAT class reductions have been suggested by Marquis et al. [5]. These penalty values represent one FAT class reduction for the specified stress ratios. All of the proposed FAT values with the penalties due to stress ratios can be found in the proposed guidelines [5].

### 3 Results and discussions

#### 3.1 Extracted fatigue data

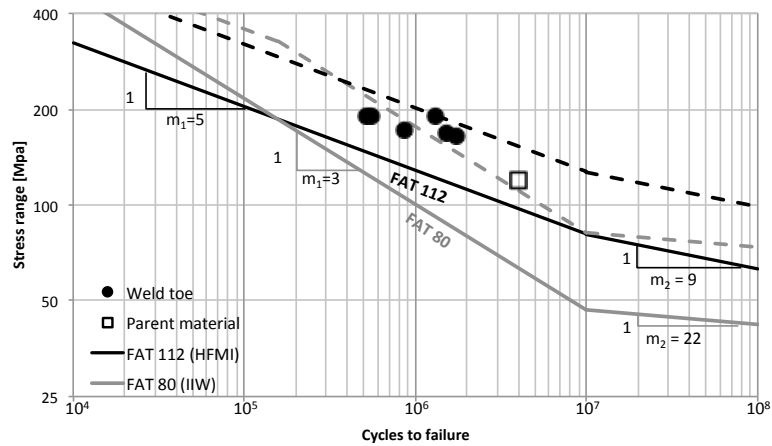
##### 3.1.1 An example demonstration from the literature

Fatigue test results obtained from Khulmann et al. [10] are considered herein for a step by step demonstration. The study included fatigue data for S690 steel grade from a stiffener detail subjected to stress ratios of  $R=0.5$  and  $R=-1$  in a large-scale beam component. As a starting point, FAT 80 representing the as-welded stiffener detail in the IIW recommendations was [3] considered. This characteristic curve is shown as a grey line in Figure 6. For the steel grade  $f_y = 690$  MPa, the guideline recommends a maximum of six (6) FAT class increase due to HFMI treatment, which corresponds to FAT 160 for  $0.15 \leq R$  [5]. As stated previously, one should apply the penalty reductions for fatigue data subjected to higher R-ratios [5]. Based on the recommendations, a three (3) FAT class reduction is expected for  $0.4 < R \leq 0.52$ . Therefore, a three (3) FAT increase in total was found as a result of both treatment and R-ratio influences. This corresponds to FAT 112 and is shown as a black line in Figure 6a. For the fatigue data obtained at  $R = -1$ , the design curve corresponds to the same S-N curve as that for  $R \leq 0.15$ , which is FAT 160. This is also shown in Figure 6b. With the exception of one single data point that failed from the parent material in Figure 6b, it is clear that previously-proposed FAT curves are conservative with respect to the available data. Probability of survival curves for 5% was also calculated for each study considering standard deviations of 0.206 for non-treated welds and 0.274 for HFMI-treated welds as presented by [20] and [7], respectively. These are shown as dashed lines in the figures.

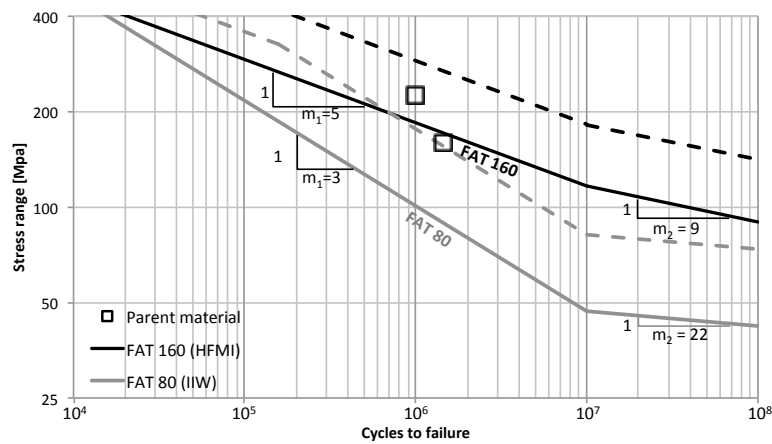
All of the S-N curves for HFMI in the guideline are assumed to have slope of  $m_1 = 5$  in the region  $1 \times 10^4 \leq N < 1 \times 10^7$  cycles and  $m_2=9$  for  $1 \times 10^7 \leq N$ . On the other hand, IIW recommended slope of  $m_2=22$  is followed for the as-welded S-N curves for  $1 \times 10^7 \leq N$ . In the following, the above mentioned assessment procedure was applied for all the fatigue



data sets extracted from the literature.



(a) Test results obtained at  $R = 0.5$



(b) Test results obtained at  $R = -1$

Figure 6: Extracted HFMI-treated fatigue data for  $550 < f_y \leq 750$  MPa from Kuhlmann et al. [10] with comparison to the design recommendations from [5]. Solid lines are considered to represent 95% survival probability and dashed lines 5% survival probability.

### 3.1.2 Further observations for other test results

According to Figure 7, all the failures for cover-plates with  $f_y = 407$  MPa failed from the treated weld toe with the exception of one data point, whereas with reference to Figure 8 only two weld toe failures were observed in the case of the stiffener details for the same  $f_y$ . Nevertheless, all the corresponding FAT curves, which are based on  $f_y$  and R-ratios, are in good agreement with the available data. Besides, the design recommendations considering AASHTO (The American Association of State Highway and Transportation Officials) curves were also given by Roy and Fisher [2]. Instead of changing the S-N slope of  $m_1 = 3$ , the recommendation for a single weld detail was composed of two sections. One design category was defined for finite regime and another was presented for infinite regime. This means that they defined various knee points for different type of weld details. This might be another way of representing the fatigue strength improvement for higher number of cycles.



In contrast to Yıldırım and Marquis [7], Roy and Fisher did not observe any material  $f_y$  effect on the fatigue strength improvement. Different design categories were only suggested based on the applied stress ratios.

The test results of Deguchi et al. [11] are presented in Figure 9. As can be seen from the figure that one point is below the proposed design curve whereas another one (run-out) fall above the proposed curve. The weld toe failure, which is below the design curve, may state that the excessive force applied after the treatment prior to fatigue testing may decrease the beneficial effects of the improvement technique. This has not been verified yet by a large number of tests of beam components. However, a similar decrease in fatigue strength was observed for longitudinal attachments in the same study considering the identical material and load history.

All of six test results of cover-plates in Figure 10 are above the proposed design curve. In this particular study, three of the cover-plates were bolted following the HFMI treatment. These are shown with a line in Figure 10. When assessing these specific test results, no distinction was made according to bolted conditions. All the data points except the one, which is run-out, are shown for the crack initiation as reported by the researchers. These samples were tested up to five million cycles and then considered as run-outs.

Figure 11 shows the results of a single test specimen that includes five cover-plate details improved by HFMI treatment. The fatigue testing was terminated when a fatigue crack had grown through the plate. Thus, all the points in the plot represent the crack initiation and they are all in the safe region.

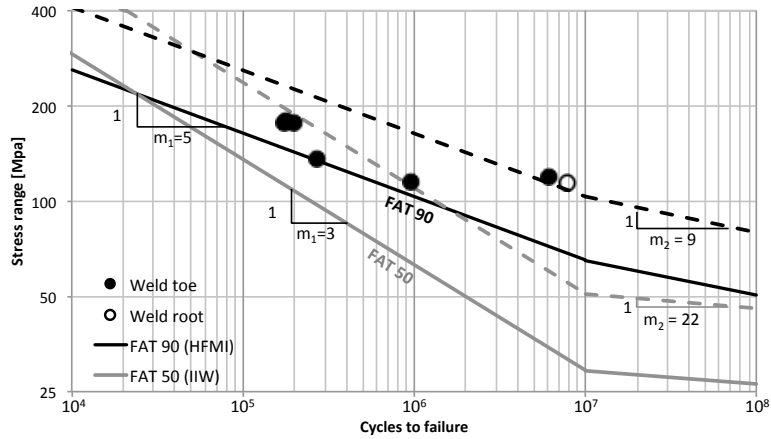
A recent study on other industrial components has been investigated in Sweden [23]. A bogie beam in an articulated hauler and a dipper arm in an excavator were considered. Schematic representations of these components are shown in Figure 12. Fatigue testing was performed for two HFMI-treated components for each case by using high strength steel of  $f_y = 700$  MPa. HFMI treatment was done on two critical weld seams around the bearing weld for the bogie beam whereas it was done on a single weld seam for the dipper arm. Two of the bogie beams and one of the dipper arms were subjected to variable amplitude loading at  $R = 0$  based on the service conditions in the field. Another dipper arm was tested under constant amplitude. According to finite element analysis of bogie beam, the critical location was the weld root of the bearing weld. For the two bogie beam components, however, cracks were initiated at the backing bar where tack welds (untreated) were present. As for the dipper arms, the starting point of the cracks were the tack welding inside the box. Thus, for all cases fatigue failures did not occur at the HFMI-treated welds, instead they moved to somewhere else. For both cases, approximately ten times improvement in life was achieved due to the HFMI treatment with respect to the as-welded states.

## 3.2 Fatigue testing of cover-plates

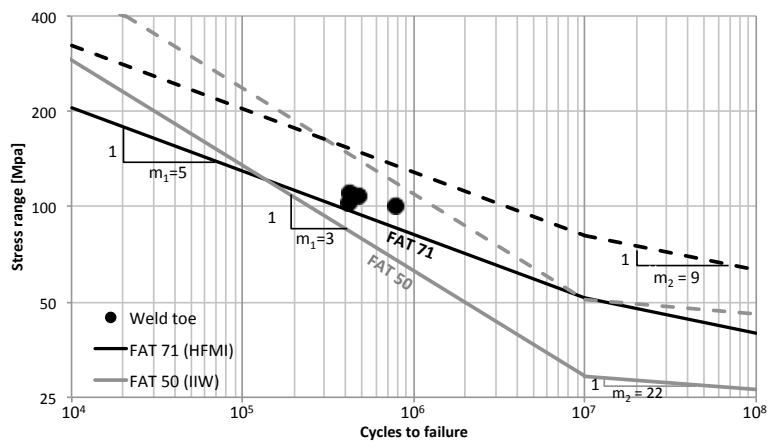
### 3.2.1 Nominal stress assessment

Fatigue test results of cover-plates performed in this study are shown for the NS system in Figure 13. The fatigue data are represented in grey and black dots for as-welded and HFMI-treated samples, respectively. For the as-welded case, the IIW recommends FAT 63 for cover-plates with a length of  $150 < L \leq 300$  mm regardless of the material yield strength

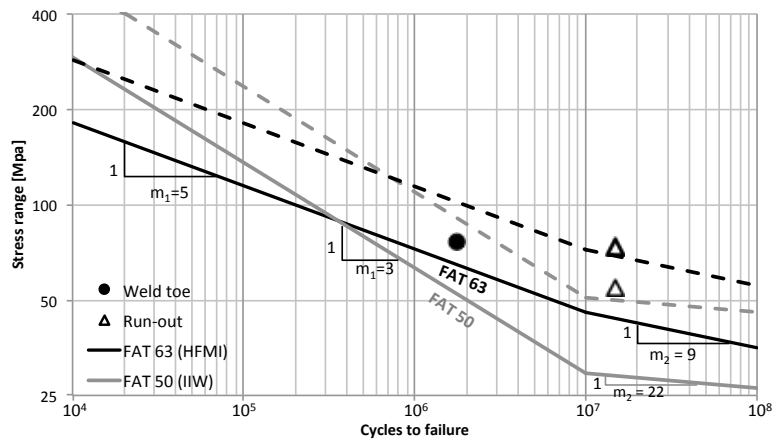




(a) Test results obtained at  $0.15 \leq R$



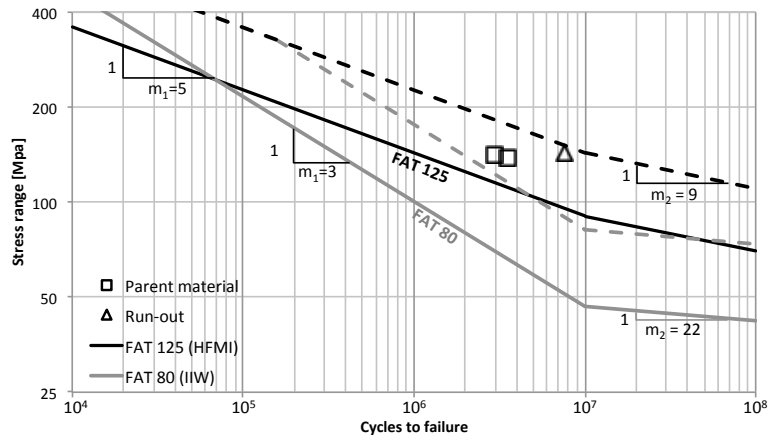
(b) Test results obtained at  $0.28 < R \leq 0.4$



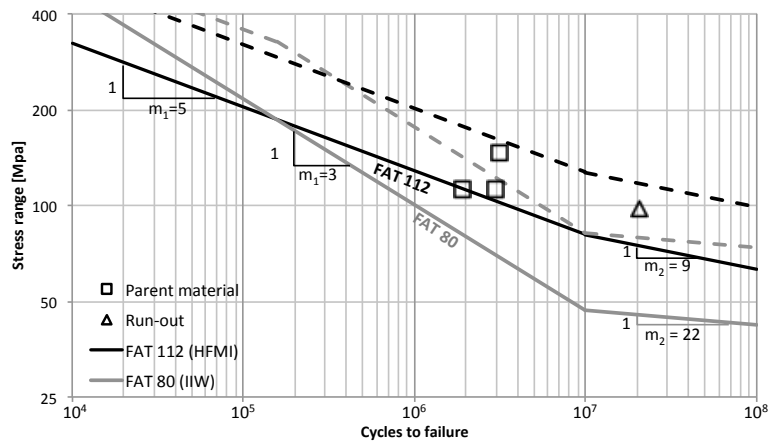
(c) Test results obtained at  $0.4 < R \leq 0.52$

Figure 7: Extracted HFMI-treated fatigue data for  $355 < f_y \leq 550$  MPa from Roy and Fisher [2] with comparison to the design recommendations from Marquis et al. [5]. Solid lines are considered to represent 95% survival probability and dashed lines 5% survival probability.

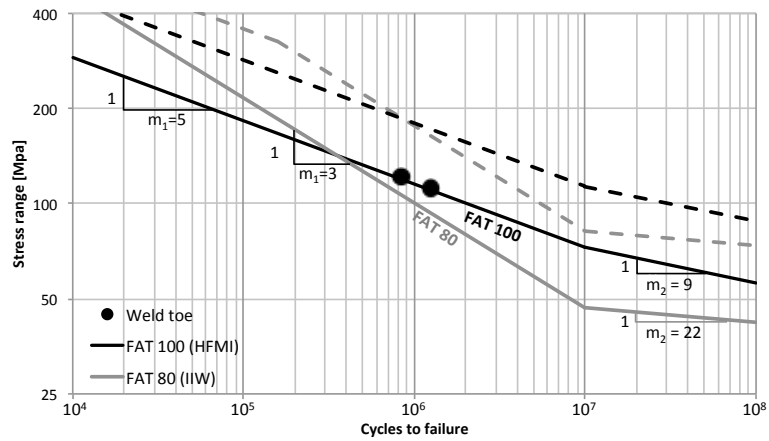




(a) Test results obtained at  $0.28 < R \leq 0.4$



(b) Test results obtained at  $0.4 < R \leq 0.52$



(c) Test results obtained at  $0.52 < R$

Figure 8: Extracted HFMI-treated fatigue data for  $550 < f_y \leq 750$  MPa from Roy and Fisher [2] with comparison to the design recommendations from Marquis et al. [5]. Solid lines are considered to represent 95% survival probability and dashed lines 5% survival probability.



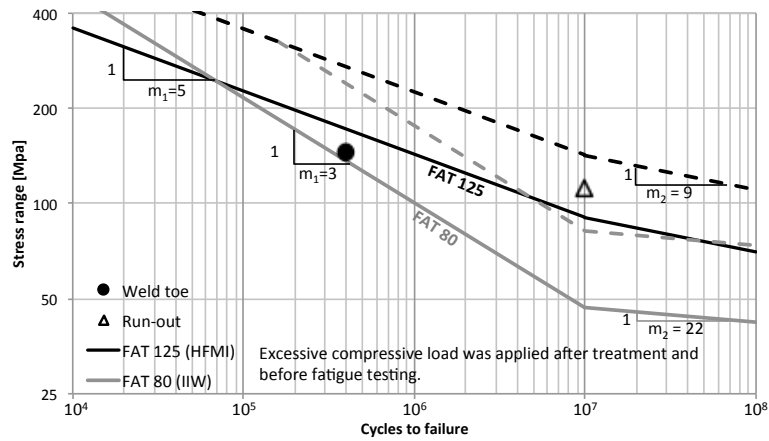


Figure 9: Extracted HFMI-treated fatigue data obtained at  $R \leq 0.15$  for  $235 < f_y \leq 355$  MPa from Deguchi et al. [11] with comparison to the design recommendation from Marquis et al. [5]. Solid lines are considered to represent 95% survival probability and dashed lines 5% survival probability.

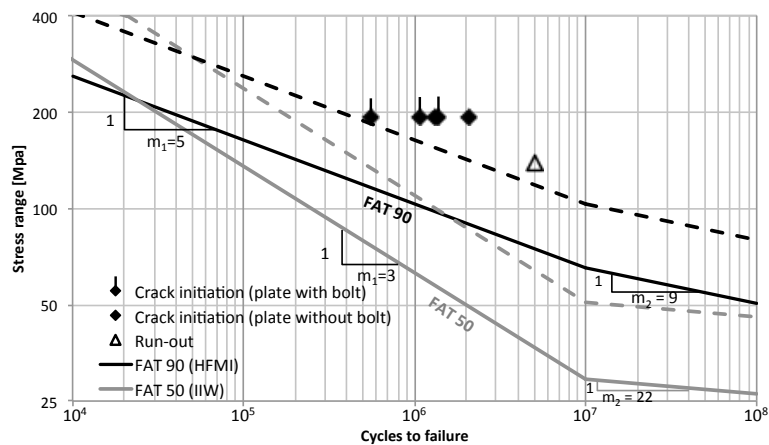


Figure 10: Extracted HFMI-treated fatigue data for  $235 < f_y \leq 355$  MPa from Vilhauer et al. [12] with comparison to the design recommendation from Marquis et al. [5]. Solid lines are considered to represent 95% survival probability and dashed lines 5% survival probability.



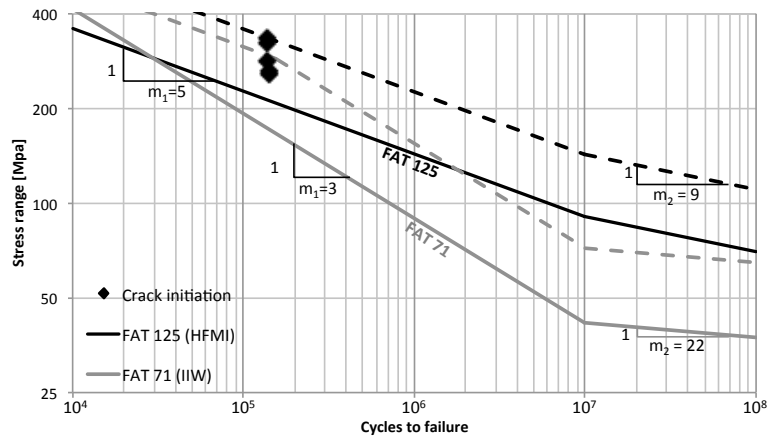
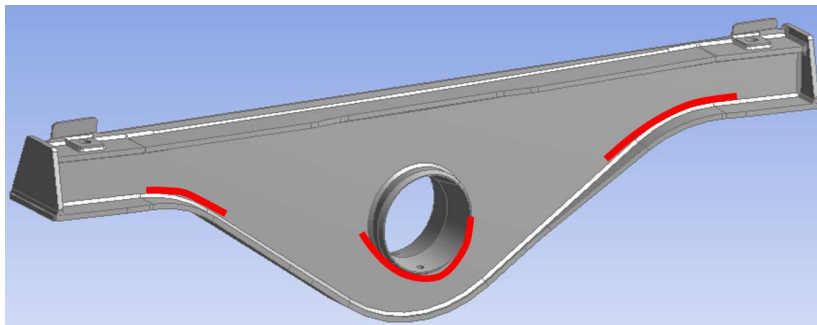
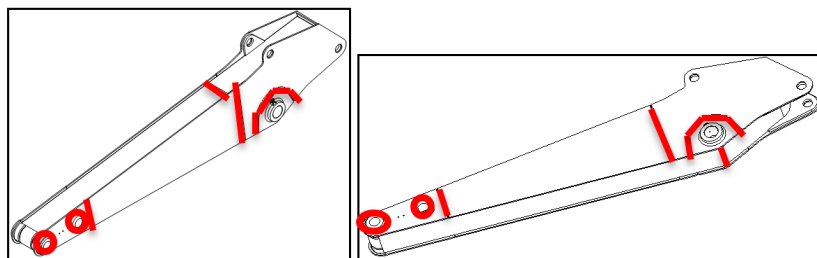


Figure 11: Extracted HFMI-treated fatigue data for  $355 < f_y \leq 550$  MPa from Lotsberg et al. [13] with comparison to the design recommendation from Marquis et al. [5]. Solid lines are considered to represent 95% survival probability and dashed lines 5% survival probability.



(a) Schematic representation of a bogie beam.



(b) Schematic representation of a dipper arm.

Figure 12: Geometries of the HFMI-treated structures from Jonsson et al. [23]. Red lines are shown for the HFMI-treated regions.



[3]. As can be seen from Figure 13 that S-N slope of the dashed grey line also changes from 3 to 5. This is because of weld details are limited by the S-N curve of the parent material, which may vary depending on the material strength [3]. In this study, with the exception of two data points, which are above the probability of survival curve for 5%, all the as-welded data remain within the scatter of grey lines. One reason for this might be that the good quality of welded high strength steel. Consequently, fatigue data points verify the usage of FAT 63 for the as-welded case.

For the HFMI-treated samples, on the other hand, the previously-proposed HFMI guideline allows a maximum of seven (7) FAT class increase for the yield strength of S900. If this is applied also for cover-plate samples, the expected characteristic fatigue strength would be FAT 140. In fact, it is clear from Figure that FAT 140 adequately represents HFMI-improved fatigue data obtained at a constant stress ratio of  $R=0.1$ .

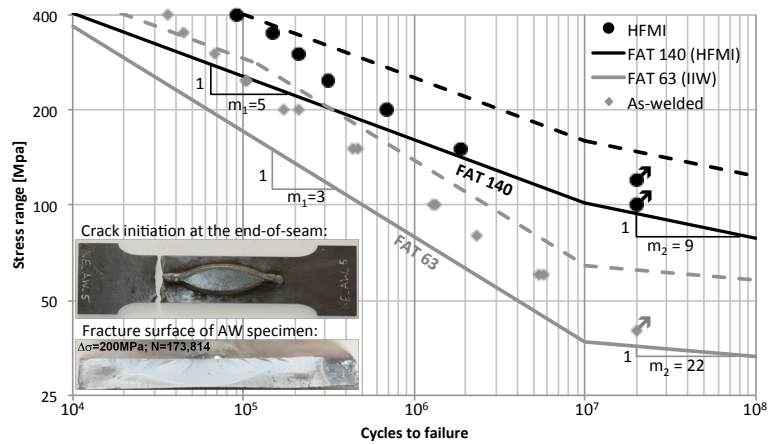


Figure 13: Fatigue test results of cover-plates performed in this study for S900.

### 3.2.2 Effective notch stress assessment

Cover-plate was modelled according to the IIW recommendations to perform stress assessment for the effective notch stress (ENS) approach. The resulting ENS concentration factor,  $K_t = 3.53$ , based on the artificial notch radius of  $\rho_f = 1$  mm at the weld toe is shown in Figure 14. Second-order solid elements were used. As recommended by Fricke [20], the maximum element size close to the weld toe and overall in the model was limited to  $R/10$  and  $1 \times t$  in all of the analyses. Weld toe angle was idealized modelled based on topographic measurements of the end-of-seam area.

Fatigue test results for the ENS approach are shown in Figure 15 with the previously-proposed corresponding fatigue design curves. These S-N curves are FAT 450 for HFMI-treated and FAT 225 for untreated joints as proposed by Marquis et al. [5] and Fricke [20], respectively. At first, the results show that the experimental data points for each condition are in good accordance to the design curves. It can be claimed that the notch stress fatigue strength of the specimens slightly exceeds the recommended and proposed values for as-welded and improved cases. Nevertheless, guidelines have to be conservative leading to a safe design and operation. One can also see that the HFMI-treated condition



shows a significant increase in fatigue strength for the investigated high-strength steel S900. Summing up, HFMI treatment offers a great potential to fulfil demands on lightweight design and furthermore ensures an efficient and safe operation.

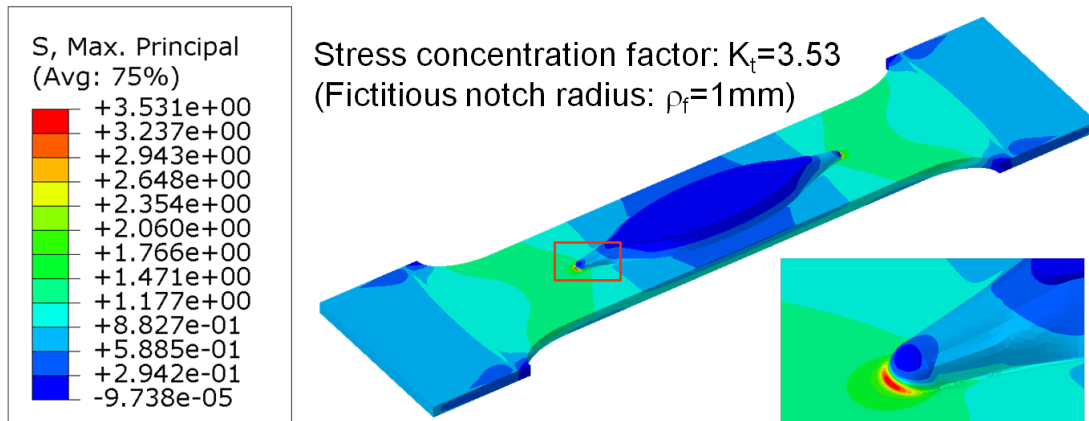


Figure 14: Calculated stress concentration value for the effective notch stress approach.

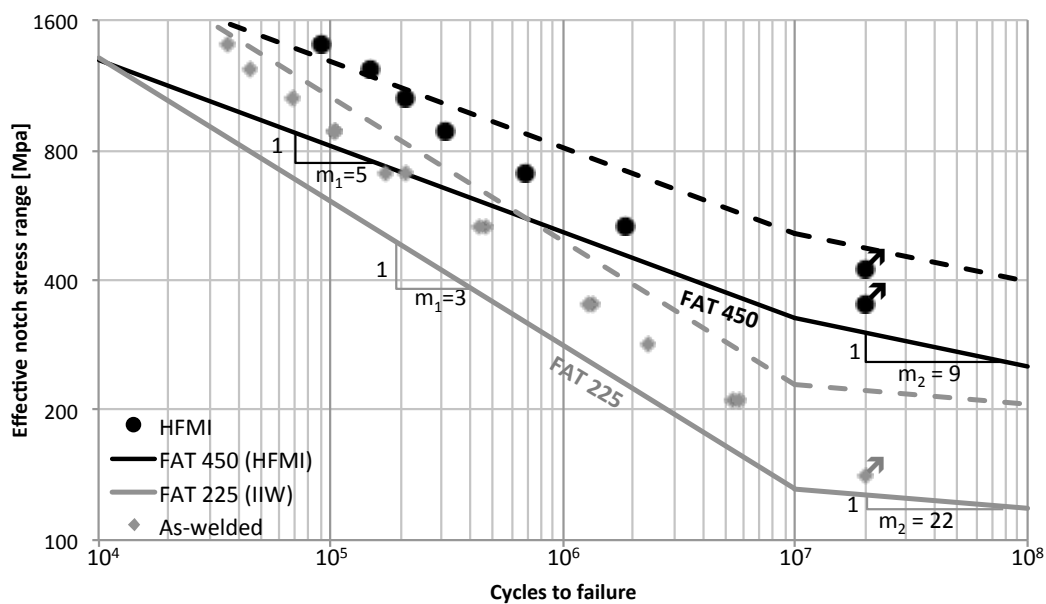


Figure 15: Fatigue test results of cover-plates in the effective notch stress range.

### 3.2.3 Typical operational load

An example of the measured strain gauge data is shown in Figure 16. The data represents load history at a minor-stressed region of the crane boom during operation. Thereby, one can see that the local stress condition exhibits distinctive variable amplitude loadings including mean stress fluctuations due to the different complex working procedures. In this study, however, fatigue tests were performed under constant amplitude loading. A recent study for



HFMI-treated welds tested under CAL and VAL states that the increase in fatigue strength under CAL, factor 3.3 at e.g.  $1 \times 10^7$  cycles, is significantly higher than for VAL, factor 1.4 respectively [24] [25]. Further fatigue tests should be performed considering VAL before FAT values are fully extended for cover-plate applications.

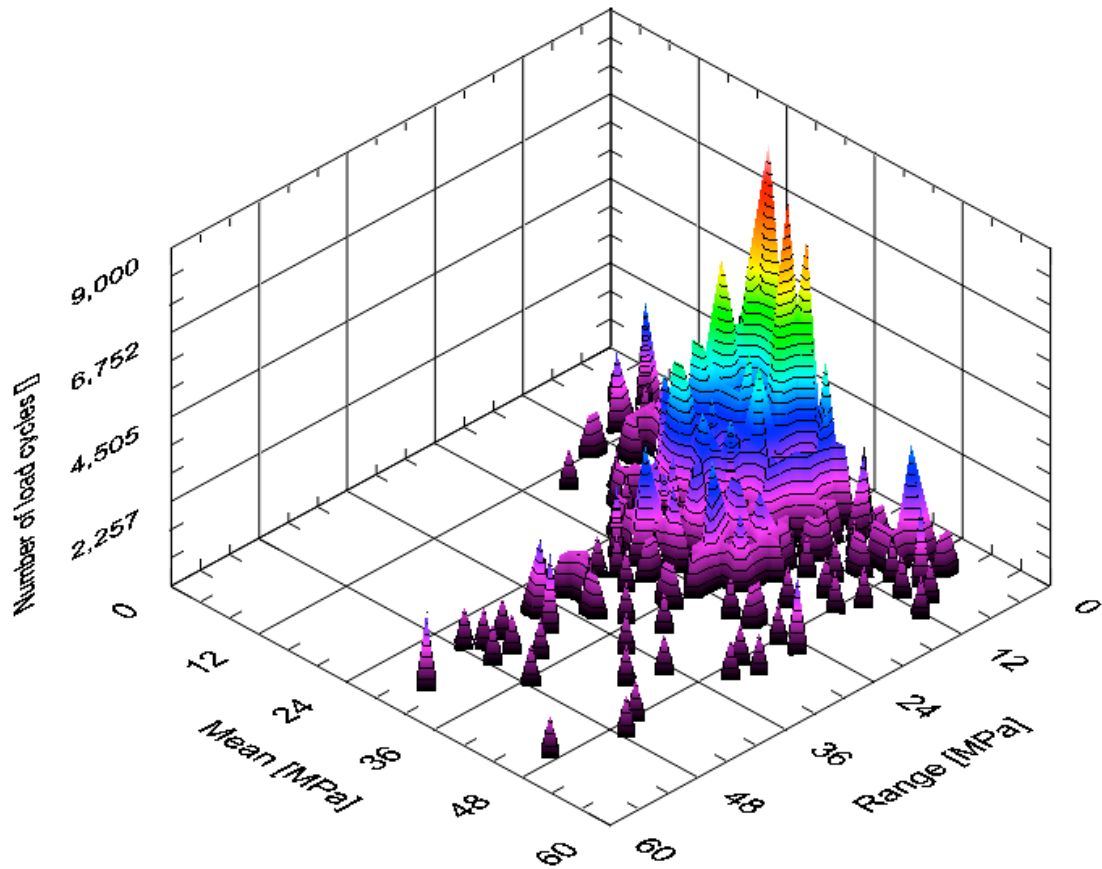


Figure 16: A typical measured strain gauge data during operation

The proposed design curves by Marquis et al. [5] were made based on test data failed at the weld toe. However, in some tests especially for large-scale structures where the treatment is not feasible at all weld toe regions, it can be commonly expected to have other types of failures, failure locations and even more run-outs. This can be observed because of shifting the critical region, e.g. weld toe, to somewhere else, e.g. parent material, after the HFMI treatment. Nevertheless, those results are also valuable and they are worth showing on a plot with respect to the design curves.

## 4 Conclusion

Experimental fatigue data extracted from the literature for HFMI-treated large-scale structures and fatigue tests carried out in this study for cover-plates have been shown with respect to the previously-proposed design curves.

According to findings following conclusion can be drawn;



1. The previously-proposed FAT classes have been verified both for the extracted fatigue data and obtained fatigue data for cover plates.
2. For the experimental test results, a local fatigue assessment method based on the effective notch stress approach has shown a good agreement in comparison with the proposed design values and it has proven the beneficial application of HFMI treatment method for a complex welded steel structure used in crane industry.
3. The degree of fatigue strength improvement based on the material strength for large-scale components are found to be consistent with the previously-proposed guidelines.
4. The previously-proposed penalty reductions in FAT classes due to high stress ratio effects have resulted in a good agreement with the extracted data.
5. In some of the studies, HFMI treatment results with very promising improvement in life even if the failure is shifted to some other locations.
6. An excessive compressive force applied after the treatment prior to fatigue testing may diminish the beneficial effect of the HFMI treatment.

## Acknowledgements

Financial support by the Finnish Cultural Foundation, the Austrian Federal Government (in particular from Bundesministerium für Verkehr, Innovation und Technologie and Bundesministerium für Wirtschaft, Familie und Jugend) represented by Österreichische Forschungsförderungsgesellschaft mbH and the Styrian and the Tyrolean Provincial Government, represented by Steirische Wirtschaftsförderungsgesellschaft mbH and Standortagentur Tirol, within the framework of the COMET Funding Programmen is gratefully acknowledged. The research presented in this paper has also been carried out as a part of the Breakthrough Steels and Applications programme within the scope of the Finnish Metals and Engineering Competence Centre (FIMECC).

## References

- [1] K. J. Kirkhope, R. Bell, L. Caron, R. I. Basu, and K.-T. Ma. Weld detail fatigue life improvement techniques. Part 1: review. *Marine Structures*, 12:447–474, 1999.
- [2] Sougata Roy and John W Fisher. Modified AASHTO design SN curves for post-weld treated welded details. *Bridge Structures: Assessment, Design and Construction*, 2:4:207 – 222, 2006.
- [3] Adolf Hobbacher. IIW recommendations for fatigue design of welded joints and components, WRC, New York, 2009.
- [4] P.J Haagensen and S Maddox. IIW recommendations on methods for improving the fatigue lives of welded joints, Woodhead Publishing Ltd., Cambridge., 2013.



- [5] Gary B. Marquis, Eeva Mikkola, Halid Can Yıldırım, and Zuheir Barsoum. Fatigue strength improvement of steel structures by high-frequency mechanical impact: proposed fatigue assessment guidelines. *Welding in the World*, 57(6):803–822, 2013. ISSN 0043-2288. URL <http://dx.doi.org/10.1007/s40194-013-0075-x>.
- [6] Gary Marquis and Zuheir Barsoum. Fatigue strength improvement of steel structures by high-frequency mechanical impact: proposed procedures and quality assurance guidelines. *Welding in the World*, 58(1):19–28, 2014. ISSN 0043-2288. URL <http://dx.doi.org/10.1007/s40194-013-0077-8>.
- [7] Halid Can Yıldırım and Gary B. Marquis. Fatigue strength improvement factors for high strength steel welded joints treated by high frequency mechanical impact. *International Journal of Fatigue*, 44(0):168 – 176, 2012. ISSN 0142-1123. URL <http://www.sciencedirect.com/science/article/pii/S0142112312001648>.
- [8] E. Mikkola, M. Dore, G. Marquis, and M. Khurshid. Fatigue assessment of high-frequency mechanical impact (hfmi)-treated welded joints subjected to high mean stresses and spectrum loading. *Fatigue and Fracture of Engineering Materials and Structures*, page n/a, 2015. ISSN 1460-2695. URL <http://dx.doi.org/10.1111/ffe.12296>.
- [9] Halid Can Yıldırım, Gary B. Marquis, and Per J. Haagenen. Experimental verification of hfmi treatment of large structures, asme 2014 33rd international conference on ocean, offshore and arctic engineering, 2014.
- [10] Ulrike Kuhlmann, André Dürr, Joachim Bergmann, and Rayk Thumser. Effizienter stahlbau aus höherfesten stählen unter ermüdungsbeanspruchung (fatigue strength improvement for welded high strength steel connections due to the application of post-weld treatment methods). Research report, Forschungsvorhaben P 620 FOSTA, Verlag und Vertriebsgesellschaft mbH., Düsseldorf, Germany, 2006. 124.
- [11] Takanori Deguchi, Masashi Mouri, Junya Hara, Daichi Kano, Taichiro Shimoda, Fumihide Inamura, Tetsuji Fukuoka, and Keisuke Koshio. Fatigue strength improvement for ship structures by ultrasonic peening. *Journal of Marine Science and Technology*, 17(3):360–369, 2012. ISSN 0948-4280. URL <http://dx.doi.org/10.1007/s00773-012-0172-3>.
- [12] Brian Vilhauer, Caroline R. Bennett, Adolfo B. Matamoros, and Stanley T. Rolfe. Fatigue behavior of welded coverplates treated with ultrasonic impact treatment and bolting. *Engineering Structures*, 34(0):163 – 172, 2012. ISSN 0141-0296. URL <http://www.sciencedirect.com/science/article/pii/S0141029611003786>.
- [13] Inge Lotsberg, Arne Fjeldstad, MortenRo Helsem, and Narve Oma. Fatigue life improvement of welded doubling plates by grinding and ultrasonic peening. *Welding in the World*, 58(6):819–830, 2014. ISSN 0043-2288. URL <http://dx.doi.org/10.1007/s40194-014-0161-8>.
- [14] SSAB. Data sheets for Domex 420 MC, Domex 700 MC and Domex 960 . Technical report, Datasheets: 11-02-03 GB8415 Domex, 11-02-03 GB8421 Domex and 11-02-16 GB8435 Domex.



- [15] Ulrich Hamme and Joachim Henkel. Neue konzepte im leichtbau – innovativer teleskopausleger eines mobilkrans. *Stahlbau*, 82(4):246–249, 2013. ISSN 1437-1049. URL <http://dx.doi.org/10.1002/stab.201310037>.
- [16] Jörn Berg and Natalie Stranghöner. Ermüdungsverhalten HFH-nachbehandelter kerbdetails des mobilkranbaus. *Stahlbau*, 83(8):553–563, 2014. ISSN 1437-1049. URL <http://dx.doi.org/10.1002/stab.201410180>.
- [17] M Leitner, S Gerstbrein, K Krautgartner, and M Stoschka. Application study of post-treated high strength steel joints in industrial crane frameworks. in: Proceedings of the IIW international conference, seoul, korea.
- [18] G Liu, Y Huang, M Gao, and Y Li. Comparison of shell and solid elements for hot spot stress analysis of complex welded joints. in: Proceedings of the twenty-first international offshore and polar engineering conference, maui, 2011.
- [19] K. Rother and J. Rudolph. Fatigue assessment of welded structures: practical aspects for stress analysis and fatigue assessment. *Fatigue and Fracture of Engineering Materials and Structures*, 34(3):177–204, 2011. ISSN 1460-2695. URL <http://dx.doi.org/10.1111/j.1460-2695.2010.01506.x>.
- [20] Wolfram Fricke. IIW recommendations for the fatigue assessment of welded structures by notch stress analysis., Woodhead Publishing Ltd., Cambridge. International Institute of Welding, Paris., 2012.
- [21] EH Moore. On the reciprocal of the general algebraic matrix. *Bulletin of the American Mathematical Society*, 26(9):394 – 395, 1920.
- [22] R Penrose. A generalized inverse for matrices. *Proc. of the Cambridge Phil. Soc*, 51:406 – 413, 1955.
- [23] Bertil Jonsson, Yang Shin, Thomas Däuwel, and Christoph Gorges. Implementing high frequency mechanical impact in industrial components: A case study. *Procedia Engineering*, 66(0):202 – 215, 2013. ISSN 1877-7058. URL <http://www.sciencedirect.com/science/article/pii/S1877705813019085>. Fatigue Design 2013, International Conference Proceedings.
- [24] Halid Can Yıldırım, Gary Marquis, and Cetin Morris Sonsino. Lightweight potential of welded high-strength steel joints from {S700} under constant and variable amplitude loading by high-frequency mechanical impact (hfmi) treatment. *Procedia Engineering*, 101(0):467 – 475, 2015. ISSN 1877-7058. URL <http://www.sciencedirect.com/science/article/pii/S1877705815006542>. 3rd International Conference on Material and Component Performance under Variable Amplitude Loading, {VAL} 2015.
- [25] M. Leitner, S. Gerstbrein, and M.J. Ottersb. Fatigue strength of hfmi-treated high-strength steel joints under constant and variable amplitude block loading. *Procedia Engineering*, 101(0):251 – 258, 2015. ISSN 1877-7058. URL <http://www.sciencedirect.com/science/article/pii/S1877705815006347>. 3rd International Conference on Material and Component Performance under Variable Amplitude Loading, {VAL} 2015.

